PHYSICAL REVIEW B

CONDENSED MATTER

THIRD SERIES, VOLUME 41, NUMBER 18 15 JUNE 1990-II

O chemisorption on Cu(110) by scanning tunneling microscopy

Y. Kuk
AT&T Bell Laboratories, Murray Hill, New Jersey 07974-2070

F. M. Chua
AT&T Bell Laboratories, Murray Hill, New Jersey 07974-2070
and Cavendish Laboratory, University of Cambridge, Cambridge, CB3 0HE, United Kingdom

P. J. Silverman
AT&T Bell Laboratories, Murray Hill, New Jersey 07974-2070

J. A. Meyer
AT&T Bell Laboratories, Murray Hill, New Jersey 07974-2070
and Brown University, Providence, Rhode Island 02912
(Received 18 January 1990)

The process of oxygen chemisorption on a Cu(110) surface has been observed dynamically using scanning tunneling microscopy. The chemisorbed oxygen is found to nucleate on terraces, and not at step edges. Isolated chains grow along the ⟨001⟩ directions after homogeneous nucleation, due to interaction anisotropy along the ⟨001⟩ and ⟨1$\bar{1}$0⟩ directions. Cu atoms diffuse in from step edges and terrace patches to form "added rows." Computer-simulation results suggest the growth mechanism of the chemisorbed layer.

I. INTRODUCTION

When a chemisorbed system has a high heat of chemisorption, a stable surface compound is formed. Ordering of this stable phase often requires the relocation of both substrate and adsorbate atoms.[1,2] The interaction of oxygen with copper surfaces is a typical example of strong chemisorption. The Cu(110)-O system has been studied for many years in order to understand the initial oxidation mechanism.[3–13] Since surface Cu atoms diffuse rapidly[14,15] at room temperature and the sticking coefficient of O is high, a well-ordered saturated (2×1) chemisorbed layer is known to form with <10 L of O [1 langmuir (L)$\equiv 10^{-6}$ Torr sec].[16] Although O atoms are known to adsorb at long-bridge sites on the Cu(110), the structure of the reconstructed Cu surface is uncertain, and the growth mechanism of the chemisorbed layer has not been known. The scanning tunneling microscope (STM) makes it possible to study the structure and the dynamics of nucleation and growth of the chemisorbed system by imaging the surface with atomic resolution as chemisorption takes place. The previously published results[11] are extended and a newly proposed structural model is described.

Molecular oxygen is known to dissociatively chemisorb on the Cu(110) surface, and the surface shows a (2×1) structure at the O saturation coverage of 0.5 ML (monolayer).[4] The chemisorption of O at the long-bridge site (twofold bridge site along the ⟨001⟩ directions) has been established by photoemission,[5] EELS (electron-energy-loss spectroscopy),[6] He diffraction,[7] SEXAFS (surface-extended x-ray-absorption fine structure),[8] LEIS (low-energy ion scattering,)[9] ICISS (impact-collision ion-scattering spectroscopy),[10] and STM.[11] Two models have been presented for the reconstructed Cu(110)-O(2×1) surface (Fig. 1): a buckled-row model in which alternate Cu ⟨001⟩ rows are displaced outward, and a missing-row model in which alternate Cu ⟨001⟩ rows are missing. The buckled-row model has been supported by HEIS (high-energy ion scattering)[12] and glancing-angle x-ray-scattering[13] data. In LEIS (Ref. 9) and ICISS (Ref. 10) measurements, the missing-row model was first proposed to explain the blocking pattern and nonexistence of a 61.8° peak in the ⟨211⟩ spectrum. Recent SEXAFS data[17] and glancing angle x-ray-scattering data[18] also favor the missing-row model due to the absence of a peak that would be present in the buckled-row model and to the measured structure factors, respectively.

Most of the studies described above have attempted to resolve the structural model at the O saturation coverage. In our previous study,[11] growth of the chemisorbed layer and the relationship between the growth mechanism and

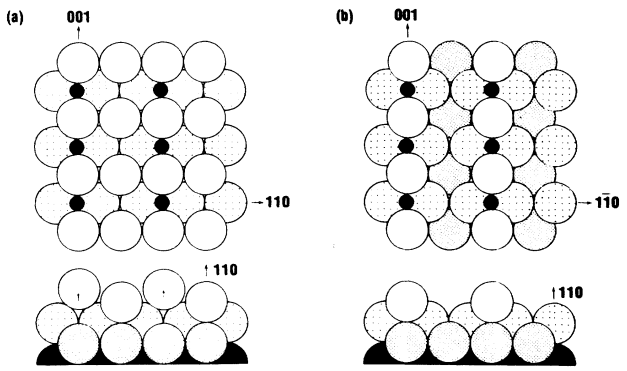

FIG. 1. Schematic diagram of the Cu(110)-O(2×1) reconstruction model. (a) Buckled-row model. (b) Missing-row model.

the structure at saturation were reported at various coverages. A new added-row model[19] of the growth mechanism of the chemisorbed layer was proposed after our previous study. In the present study we show experimental evidence to support the added-row model. The added- and missing-row models result in an identical surface at saturation coverage, so the present results also agree well with recent studies[17,18] of the saturated structure. The growth mechanism was studied by the coverage dependence of the STM images. Computer-simulation results, based on a lattice-gas model, are compared with the STM observations.

II. EXPERIMENT

A detailed description of the tunneling microscope used in this study can be found elsewhere.[20] The instrument is housed in an ultrahigh-vacuum (UHV) chamber with an operating pressure of 1×10^{-10} Torr. After electrochemical polishing, the Cu(110) single crystal with $<0.5°$ miscut was prepared by successive ion-sputtering and annealing cycles until a clean (1×1) surface was imaged by the STM with a W tunneling tip. The sample was annealed at ~300 °C for >6 h before O exposure in order to obtain large terraces with straight step edges.[21] On a clean Cu(110) surface, $\langle 1\bar{1}0\rangle$ Cu rows were observed with corrugations of <0.03 Å, but individual Cu atoms in these rows were not resolved. For the chemisorption experiment, oxygen was admitted via a short tube with a 0.16-cm orifice, 3 cm away from the sample surface with the instrument in its tunneling position. In this way the dynamic response of the surface upon arrival of the gas could be observed. It also allowed precise control of the coverage; a chemisorption rate [(sticking coefficient)×(flow rate)] of 0.001 ML/sec was easily achieved. The coverage was determined by counting the number of O-containing rows observed in several large-area STM images.

The spatially resolved electronic structure of the surface was acquired by periodically measuring $(V/I)dI/dV$ versus V during a constant-current topography scan.[22] This method makes it possible to correlate the local density of states with a particular topographic feature, while reducing the probability of changes in the tunneling tip that could occur during consecutive topographic and spectroscopic scans.

III. STRUCTURE OF Cu(110)-O(2×1)

Three structural models have been proposed for the Cu(110)-O(2×1) surface: added, missing, and buckled rows. In the recently proposed added-row model[19] (Fig. 2), a Cu terrace is regarded as a lattice-gas system and a step edge is considered as a two-dimensional (2D) fluid-gas interface. Extra Cu atoms (on top of the first layer), with a high room-temperature diffusivity,[14,15] move along the $\langle 1\bar{1}0\rangle$ direction and become bound to diffusing O atoms to form a row along $\langle 001\rangle$, as shown in Fig. 2(a) with the O in the preferred long-bridge site (B') of the added row. An O atom weakly bound at the asymmetric bridge site (B) at the end of the added row will have its chemisorption energy lowered by a Cu atom binding to the site labeled A. The long-bridge site in the added row is preferable to that on the first layer; the added Cu atoms (the first-nearest neighbor for O) bond more stably, perhaps by a small vertical displacement. A STM image of the Cu-O added row would appear as a protrusion due to the increase of charge density. In the missing-row model (Fig. 3), as O atoms are chemisorbed at the long-bridge sites of the first layer, Cu atoms in the adjacent $\langle 001\rangle$ rows [e.g., sites C, C', D, and D', in Fig. 3(a)] must diffuse away along $\langle 001\rangle$. A STM image would show troughs (decrease in charge density) near adsorption sites. In the buckled-row model the chemisorbed O causes alternate Cu $\langle 001\rangle$ rows to buckle outward, Unlike the missing- and added-row models, no mass transport of Cu atoms is required.

The surface structures of the added- and missing-row models are identical at saturation coverage (0.5 ML), as shown in Figs. 2(b) and 3(b). They are, however, quite different at partial coverages [Figs. 2(a) and 3(a)]. There-

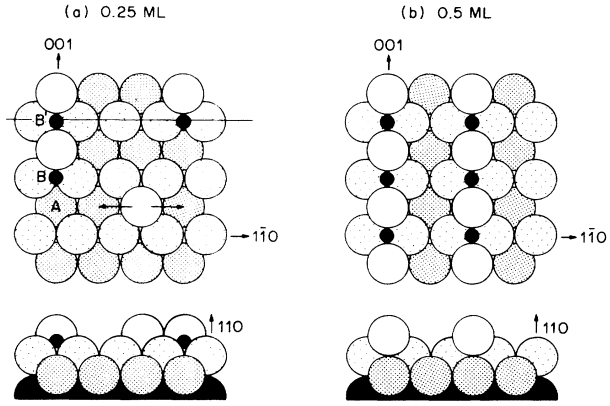

FIG. 2. Schematic diagram of the added-row model of Cu(110)-O(2×1). (a) As O atoms bind with diffusion Cu atoms (indicated by arrow) at 0.25 ML, they form an added row along $\langle 001\rangle$. (b) At saturation coverage this model is identical to the missing-row one. A line is drawn to indicate registry, as in Fig. 4.

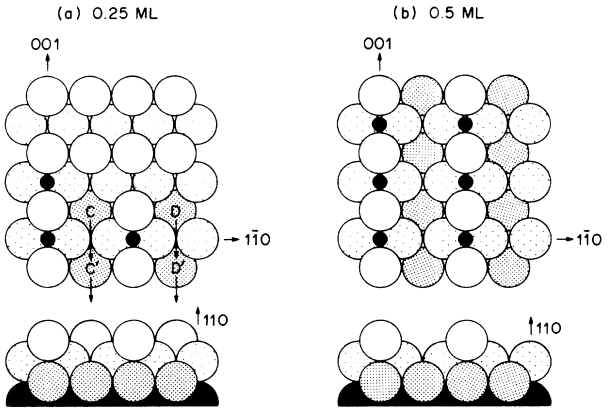

FIG. 3. Schematic diagram of the missing-row model of Cu(110)-O(2×1); (a) as three O atoms adsorb at 0.25 ML, four Cu atoms diffuse away from the area as indicated by arrows, and (b) at saturation coverage.

fore, in order to determine the correct structure model for Cu(110)-O(2×1), atomic-resolution STM images taken at various coverages are needed. The low-coverage (0.05 ML) scan shown in Fig. 4 is useful in determining both the registry and height of the O-induced rows with respect to the substrate. The image reveals the ~0.03−Å corrugation of the bare ⟨1$\bar{1}$0⟩ rows of the unreconstructed level as well as the bright lines of spots indicating the O-induced ⟨001⟩ rows. The spots are in exact alignment with the underlying ⟨1$\bar{1}$0⟩ rows. Using the Cu terrace steps (1.28 Å) for calibration, the O-induced rows appear to protrude vertically by 0.8±0.2 Å from the bulk position. (The variation in the measured vertical height with gap voltage is reflected in the uncertainty of 0.2 Å. The 0.8-Å protrusion is discussed further below.)

Observation of the growth of the O-induced rows, with increasing O exposure, provides further information for use in choosing the correct structural model. With increasing O coverage, isolated rows on terraces grow along ⟨001⟩. The rows form more readily on small terraces than on large ones, implying that their growth was limited by diffusion of Cu atoms from step edges. The buckled-row model is thus eliminated, since it does not require mass transport and would therefore not have a diffusion-limited growth character. If the missing-row model were the correct description, missing rows would be observed next to O chemisorption sites. This was not observed in Fig. 4 or in any other images, ruling out this model. Therefore, the added-row model is the correct structural description, and the bright spots in the O-induced row of Fig. 4 represent O atoms in the added row as shown by the solid line in Fig. 2(a).

With ~10 L of O exposure, a (2×1) structure was formed on most of the surface. Figure 5 shows STM images taken at gap voltages of −1 and +1 V. Bright spots show a 5.1×3.6-Å^2 unit cell, forming a (2×1) reconstruction. The resolution of the STM images at the tunneling voltage of −1 V is better than at +1 V, indicating that both geometric and electronic structure influence the STM images. Measured corrugation (vertical height between sites *P* and *Q*) of the bright spots was found to depend strongly on the tunneling-tip size. The measured 0.8-Å apparent protrusion of the added row above the substrate therefore cannot be taken literally as the actual

FIG. 4. 35×26-Å^2 gray-scale image at 1 V. Two solid lines are drawn to indicate the registry of the O atom with underlying Cu atoms. Spectra taken at sites *A*, *B*, and *C* are shown in Fig. 6.

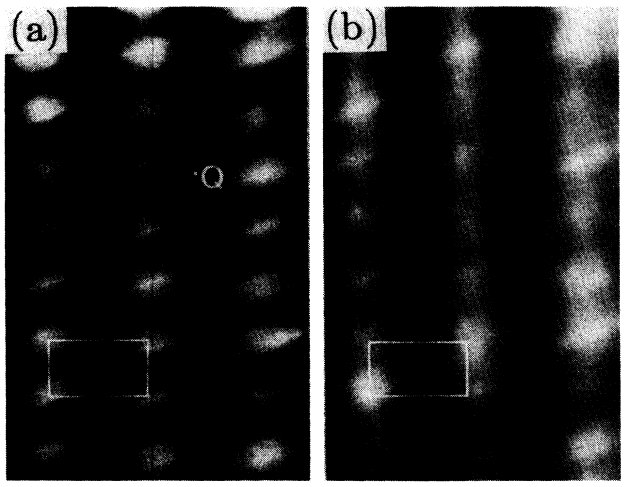

FIG. 5. 29×15.5-Å^2 gray-scale images of a Cu(110)-O(2×1) surface at (a) −1 V and (b) 2 V. (2×1) unit cells are marked.

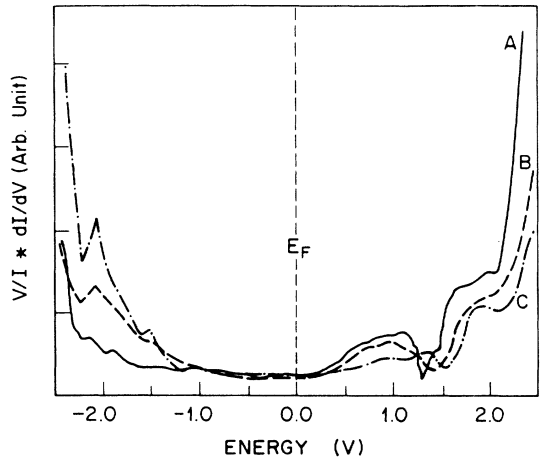

FIG. 6. Normalized tunneling conductance at sites *A* (solid line), *B* (dashed line), and *C* (dotted-dashed line) of Fig. 4.

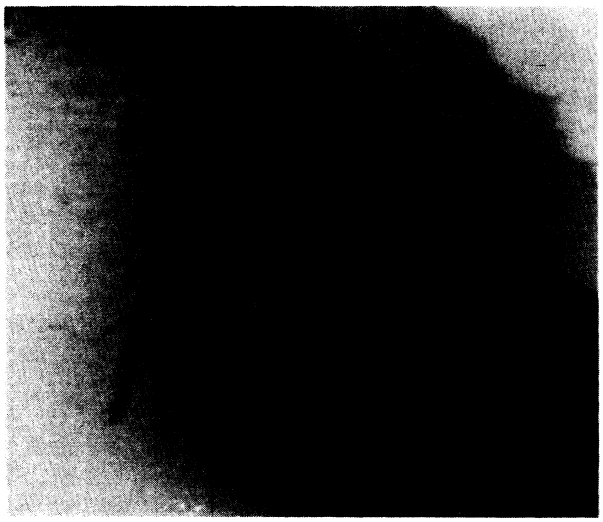

FIG. 7. 120×90-Å^2 image at +1 V. The O row appears as a trough due to the O-chemisorbed W tip.

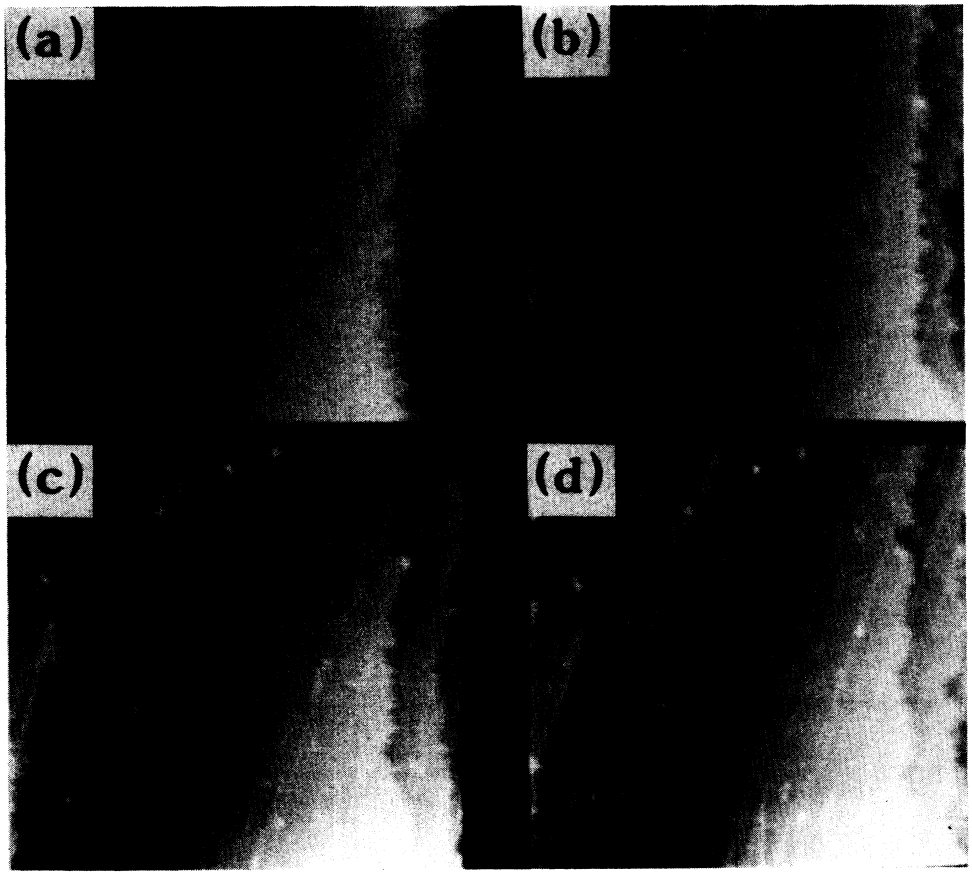

FIG. 8. 600×480-Å^2 images at −1 V on (a) clean surface, and at (b) 0.02 ML, (c) 0.06 ML, (d), 0.09 ML, (e) 0.17 ML, (f) 0.20 ML, (g) 0.30 ML, and (h) 0.40 ML coverage. Patches are indicated by small arrows. Large arrows in (e)–(g) indicate the same patch growth with increasing O coverage.

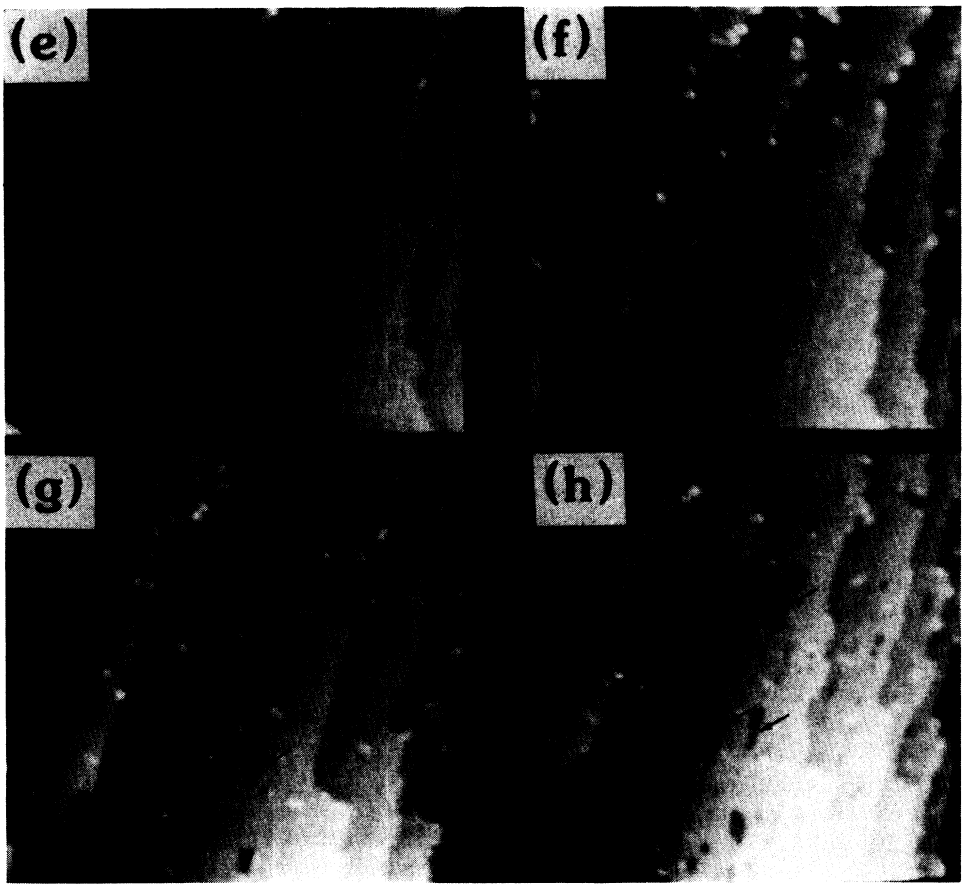

FIG. 8. (*Continued*).

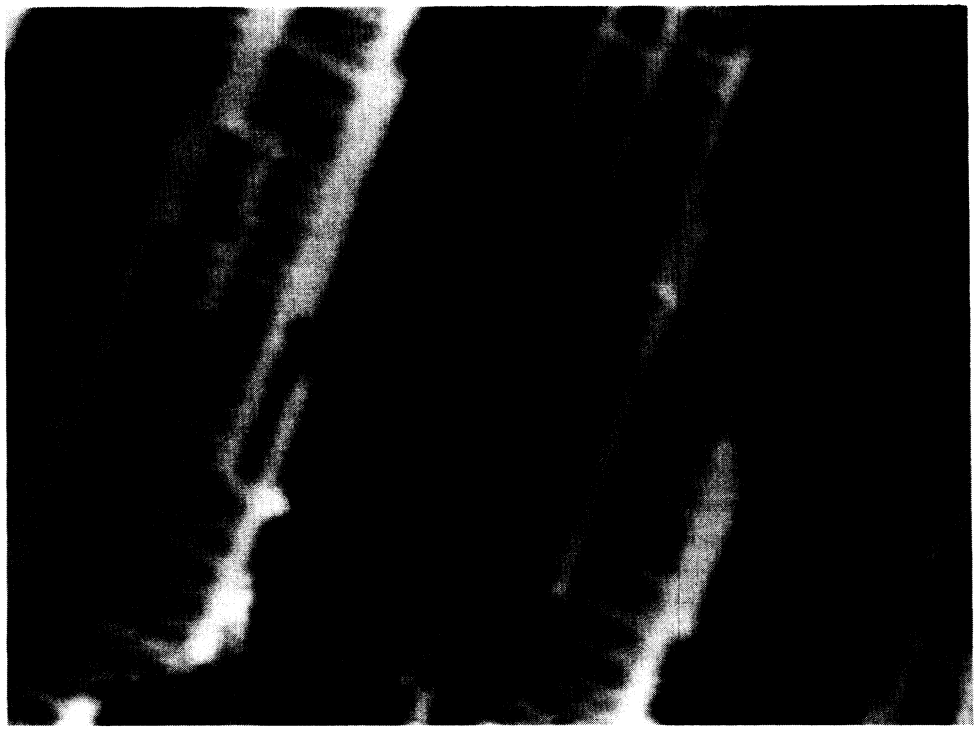

FIG. 9. 240×190-Å^2 images at 0.2 ML O. Protrusions along $\langle 1\bar{1}0 \rangle$ are shown by arrows.

vertical height of the O atoms above the underlying Cu plane. Previous measurements by other techniques give conflicting values for the height. A SEXAFS measurement[17] suggests that the O is situated 0.35 Å above the long-bridge site of the added row, while glancing-angle x-ray-scattering results[18] indicate that the O is buried 0.34 Å below the long bridge, with 0.37 Å outward displacement of the added row. Considering the first- and second-nearest neighbors, the long-bridge site on the added row is equivalent to that on the first layer, so there must be another reason for the preferred, chemisorption of the O atom on the added row. A recent theoretical study[23] suggested that the O $2p$ state hybridizes more strongly with Cu d states on metal atoms with a low metal coordination number. Therefore, the long-bridge sites on the added row are energetically more favorable than that on the first layer for O chemisorption. The study also indicated that O is buried slightly below the long-bridge sites of the added row.

Scanning-tunneling-spectroscopy (STS) measurements were made at different sites on the surface in order to confirm the presence and position of the adsorbed O on the added rows. Figure 6 presents $(V/I)dI/dV$ curves at three sites indicated in Fig. 4: on the unperturbed site A; above the adsorbed O atom, site B, and at the first-nearest-neighbor Cu atom, site C. Didio *et al.*[5] and Courths *et al.*[24] have reported that the electron state density from 1 to 2 eV below E_F increases due to the presence of Cu—O antibonding states along the ⟨001⟩ chain, while the Cu $3d$ states around -2.5 eV decrease upon O chemisorption. The higher state density below -1 eV in the curves at B and C confirms the previously proposed O chemisorption site and antibonding states. Since antibonding states have nodal structures in real space, the measured charge density on the nodes would be lower than that on the other area. As shown in Fig. 5, the better resolution was obtained at a gap voltage of -1 V rather than $+2$ V. Photoemission and inverse-photoemission data have located surface states in the s-p band gap from $\bar{Y}$ to $\bar{\Gamma}$.[25,26] STS measures the local density of states summed over **k** vectors with varying weighting factors due to different decay lengths at various **k**. If the states are dispersive like image states, the width of the state in the tunneling spectrum can be a measure of the dispersion. In the curve at A, the peaks centered at ~ 0.8 and ~ 1.8 eV of width ~ 1.0 eV agree with the dispersion of the Shockley states calculated by Chen and Smith.[27] The surface states are smaller in curves at B and C, but the shift of the peaks is less than in the results reported from inverse photoemission.

In a recent study of O chemisorption on Al(111),[28] it was reported that the measured STM images of sample empty states of O atoms changed from protrusions to holes as the gap voltage was changed. We were able to observe such dependence only when the tunneling tip was apparently contaminated by O adsorption. Figure 7 shows O-induced rows which appear as troughs instead of protrusions. Tunneling spectroscopy in this case showed a large energy gap (larger than 1.5 eV). After the tip was cleaned by field emission (tunneling current > 100 nA), the images of troughs changed to protrusions at tip voltages from -3 to $+3$ V, and the gap in STS was not observed.

IV. GROWTH KINETICS

In order to understand the dynamics of the chemisorption process, tunneling images were taken at various coverages up to 0.5 ML. Figures 8(a)–8(h) show STM images of the same area on a clean Cu(110) surface and increasing coverage of O up to 0.4 ML. The time interval between consecutive images varied from 2 to 10 mins, so adjustment of the x-y position was often necessary to compensate for thermal drift. On a clean surface in Fig. 8(a) the step edges appeared to be unusually rough compared to those on other metal surfaces.[29,30] As discussed in the preceding section, step edges can be treated as a fluid-gas interface in a lattice-gas model.[31] In this model the concentration of diffusing Cu atoms is determined by the evaporation energy (W_s) from the step edge onto a terrace; $n_{ad} = n_0 \exp(-W_s/kT)$, where n_{ad} is the concentration of extra adsorbed Cu atoms diffusing on the terrace and n_0 is the prefactor which includes an entropy term. The equilibrium among step edges, terraces, and vacuum is the result of two separate processes: (i) diffusion of extra Cu atoms from and toward the steps and exchange with them, and (ii) diffusion of Cu atoms in the edge of the steps toward kinks and exchange with them. Cu atoms are known to diffuse more rapidly along ⟨1$\bar{1}$0⟩ than along ⟨001⟩.[15] Since most observed steps are close to the ⟨001⟩ direction in Fig. 8(a), process (i) takes place more easily than process (ii), resulting in the roughness of the step edges. Images of various-sized areas showed the same mean displacements in the edge, confirming that the raggedness of the edges was a real effect and not due to scanning noise. When O-induced rows formed on a terrace, they acted as a diffusion barrier to extra Cu atoms because they are aligned along ⟨001⟩, so the diffusion coefficient along ⟨1$\bar{1}$0⟩ is reduced. When part of a step edge was terminated by an O-induced row, diffusion of Cu atoms from and toward that area was reduced. In Fig. 8(d), the step edges that are terminated by

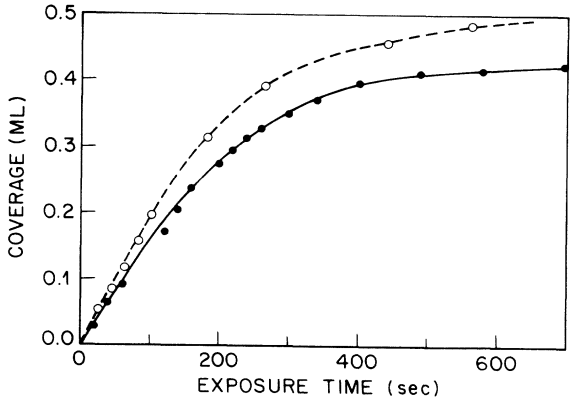

FIG. 10. O coverage as a function of O exposure time on surfaces with average step widths of 150 Å (solid circle) and 50 Å (open circle).

O-induced rows are perfectly straight while those without them remain rough.

Figure 8(b) shows an image taken at 0.025 ML O coverage. Isolated O-induced rows >25 Å long began to appear on Cu terraces, but not near step edges. When consecutive STM images were taken of this area at the same coverage, rows shorter than that length seemed to coalesce or break apart (shown by arrow). That length, therefore, seems to be critical for homogeneous growth. While most O-induced rows followed the homogeneous

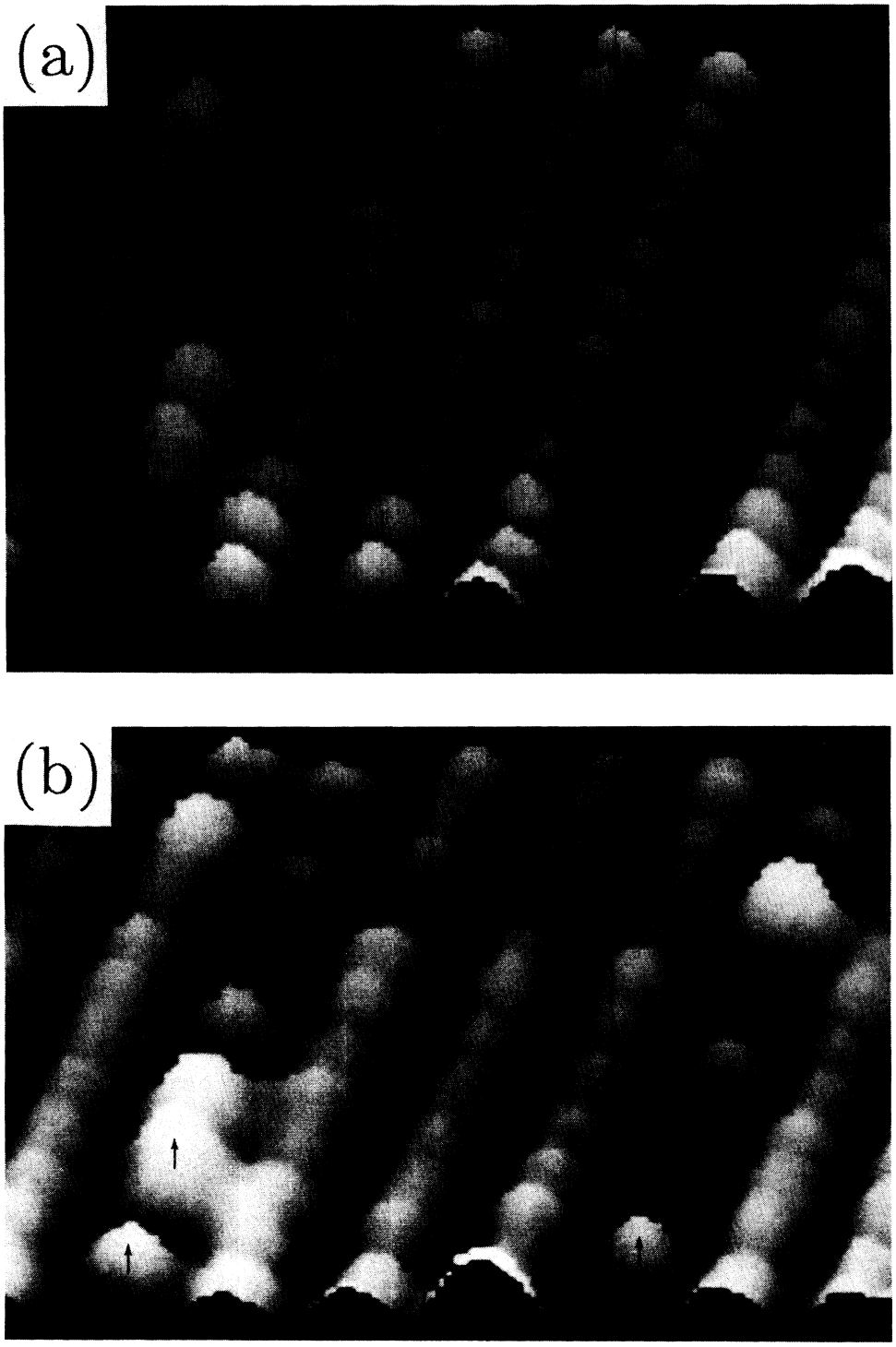

FIG. 11. 120×90-Å^2 images at (a) -1 V and (b) 2 V. The atoms indicated by arrows disappear at -1 V.

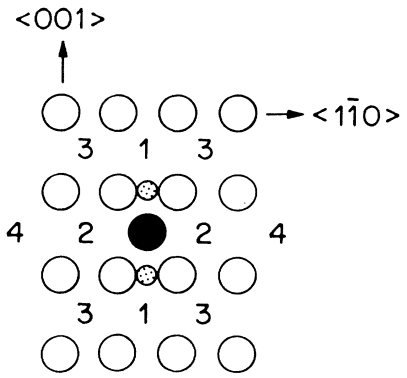

FIG. 12. Constraint used in the computer simulation (see text).

nucleation mechanism, some rows seemed to nucleate and grow around defects. The change of the step edges due to O adsorption (advance of steps or change of kinks) could be observed with additional O exposure. However, the shapes of some step edges changed with time even without introducing more O, indicating that the gain or loss of atoms at step edges is not due to O adsorption alone. As the coverage increased, the isolated O-induced rows grew along $\langle 001 \rangle$, some up to several hundred Å long. At low coverages, they remained separated, without forming (2×1) islands. The distances between rows corresponded to 3×1, 4×1, 5×1,.... Since the coherence length for LEED is longer than this local ordering, surfaces such as those shown in Figs. 8(c) and 8(d) cannot show the corresponding long-range order, but streaks along $\langle 1\bar{1}0 \rangle$ at low coverage have been previously reported.[3]

As the coverage reached about 0.2 ML [Figs. 8(e), 8(f), and 9], protrusions along $\langle 1\bar{1}0 \rangle$ began to appear perpendicular to the O-induced rows, like rungs in a ladder (shown by arrows). STS on top of these protrusions was very similar to that on clean Cu(110), indicating that they were $\langle 1\bar{1}0 \rangle$ rows in the first layer below the added rows that had buckled outward to relieve strain. These "strain lines" were separated by $n\mathbf{a}_{\langle 001 \rangle}$, where n is an integer, with an average height of $\sim$0.1 Å. The clean Cu(110) surface is known to have mutilayer relaxation with a first-layer contraction of $\sim$0.1 Å.[32,33] When the separation between two O-induced rows was larger than $5\mathbf{a}_{\langle 110 \rangle}$, the strain lines did not appear. The displacement appears to be the same magnitude as the contraction of the first layer on a clean surface, indicating that the first-layer contraction is undone at this coverage.

At $\sim$0.3 ML, rectangular patches of missing first-layer Cu atoms began to appear. They increased in size very slowly with additional O exposure. They were also bounded on two sides by the O-induced rows, attesting to the barrier the reconstruction provides for removal of more Cu atoms. Oxygen atoms require added Cu to stabilize their position. If Cu atoms are not available from step edges on a large terrace or step edges are terminated by O-induced rows, Cu atoms are apparently supplied from these patches, though much more slowly than from step edges at low coverage. Figure 10 shows the depen-

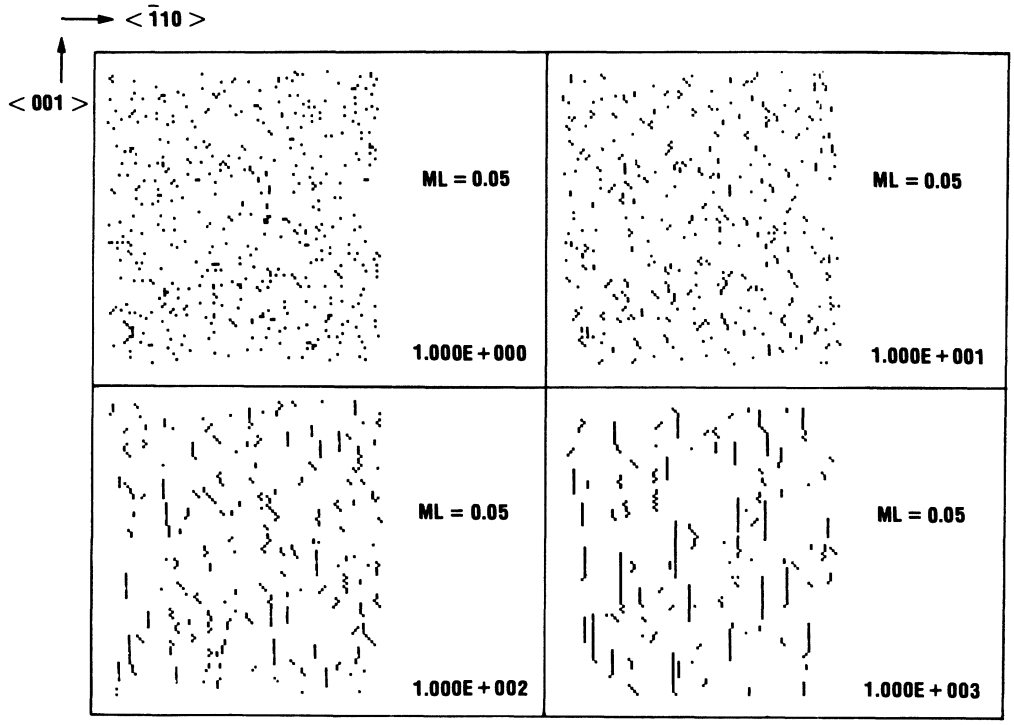

FIG. 13. Simulated images of added rows at 0.05 ML, after four different elapsed times.

dence of measured O coverage on the O exposure time. (The same flow rate was used for all coverages.) The slope is proportional to the O sticking coefficient. The solid circles indicate the data of O adsorption on terraces with an average width of ~150 Å, and the open circles those terraces with average width of ~50 Å. The dependence of the sticking probability on the coverage does not follow simple Langmuir kinetics. The initial sticking coefficient is higher on a surface with high step density, again proving that step edges serve as sources of the diffusing Cu atoms. The sticking coefficient decreases at an O coverage of 0.2–0.3 ML on surfaces both with small and large terraces. At this coverage added rows are abundant and act as diffusion barriers. Without added Cu atoms, adsorbed oxygen cannot be stabilized, so the sticking coefficient decreases. Oxygen atoms adsorb more slowly by forming added rows with the Cu atoms from the patches. The asymptotic value for O coverage on large terraces is less than 0.5 ML, as shown in Fig. 10. When the primary adsorption sites are no longer available for O due to unavailability of extra Cu atoms, secondary adsorption sites began to appear in STM images (Fig. 11). The atomic images[34] of these sites were strongly voltage dependent. Tunneling spectroscopy showed characteristic peaks at ~+2.0, −1.0, and −2.0 eV, different from those on the primary adsorption sites.

In order to better understand the growth observations, a Monte Carlo simulation was performed. A lattice-gas model is assumed in which the number of added Cu atoms determines the coverage and the number of O atoms is determined. The displacement for each time interval is adjusted by varying the diffusion constant. Since details of the dissociation of O_2 molecules and the diffusion of O atoms are not yet known (no precursor state has been observed), O atoms are assumed to diffuse much faster than the Cu atoms when they are not bound to a Cu-O chain. However, once an O atom is attached to an added Cu-O chain, its probability to diffuse away from the Cu-O pair is assumed to be low. O atoms are allowed to be situated on top of the short-bridge sites of the first layer (equivalent to the long-bridge sites in the added row), while Cu atoms occupy fourfold-hollow sites, by the proposed structural model. A constraint for the simulation is illustrated in Fig. 12. As a Cu added atom is bound to two O atoms, site 1 is more favorable for an additional added Cu atom than any other site, as described earlier. Site 2 is the least favorable since the O-O distance is too small (2.55 Å) if two neighboring Cu-O chains are formed. It was found from the simulation that this is the only constraint required to produce anisotropic growth in equilibrium. It is known that the adatom surface diffusion is anisotropic on Cu(110) ($D_{110} > D_{001}$),[15] but the ratio of the anisotropy does not influence the equilibrium structure. Diffusion anisotropy results in anisotropic growth only in a diffusion-limited process. Figure 13 shows the simulated Cu-added-atom movement as a function of time, using the diffusion constant of Ag on Cu(110) for self-diffusion.[15] After 1 msec, the simulated images resemble the STM image [Fig. 8(c)]. (The resemblance is better after 1 sec.) The best fits of various parameters were determined from visual comparison of the simulated result to the corresponding STM images. However, the following conclusion is derived from wide variation of the parameters. The 1D Cu-O chain growth is obtained due to the anisotropic interaction. In Figs. 8(b)–8(d), homogeneous nucleation with a critical nucleation length was observed. The critical length is determined by the difference in the desorption energies of Cu atoms from the end and from the middle of the Cu-O chain. From the simulation, it was found that ~0.14 eV is required to remove a Cu atom from the end of the Cu-O chain, while ~0.16 eV is needed from the middle of the chain at room temperature. The results at various O coverages are shown in Fig. 14. At low coverage the growth is mainly governed by the formation energy of the Cu-O chain. With increasing coverage, the Cu-O chains act as a diffuion barrier of added Cu atoms, resulting in diffusion-limited growth.

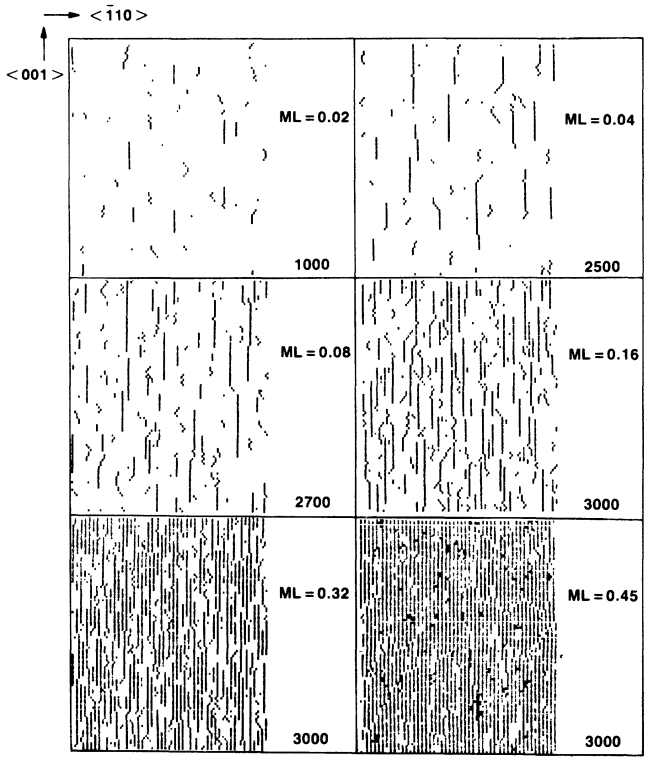

FIG. 14. Simulated images of added rows at six different coverages.

V. CONCLUSION

Cu atoms on the Cu(110) surface diffuse rapidly even at room temperature, and are stabilized with dissociated O atoms, forming added Cu-O atomic rows preferentially along ⟨001⟩. Once the rows reach a critical length, they grow further; at shorter lengths they break apart. The added-row model, a newly proposed structural model, is equivalent to the missing-row model at saturation coverage (0.5 ML). Therefore, this model supports most previously reported results at 0.5 ML obtained by other techniques. The coverage dependence of the O sticking coefficient and of the STM images implies a diffusion-

limited process as the added row acts as a diffusion barrier. A second adsorption site begins to appear on large terraces at 0.4 ML. Scanning tunneling microscopy and spectroscopy has been used to resolve successfully both the structure and growth mode of a surface.

ACKNOWLEDGMENTS

The authors acknowledge helpful discussions with W. L. Brown, C. T. Chen, P. H. Citrin, P. J. Estrup, I. K. Robinson, N. V. Smith, R. F. Willis, and D. M. Zehner.

[1]G. Somorjai, *Physics and Chemistry of Surfaces* (Academic, New York, 1980).
[2]A. M. Baro, G. Binnig, H. Rohrer, Ch. Gerber, E. Stoll, A. Baratoff, and F. Salvan, Phys. Rev. Lett. **52**, 1304 (1984).
[3]G. W. Simmons, D. F. Mitchell, and K. R. Lawless, Surf. Sci. **8**, 130 (1967).
[4]G. Ertl, Surf. Sci. **6**, 208 (1967).
[5]R. A. Didio, D. M. Zehner, and E. W. Plummer, J. Vac. Sci. Technol. A **2**, 852 (1984).
[6]J. A. Stroscio, M. Persson, and W. Ho, Phys. Rev. B **33**, 6758 (1986).
[7]J. Lapujoulade, Y. Le Cruser, M. Lefort, Y. Lejay, and E. Maurel, Phys. Rev. B **22**, 5740 (1980); Surf. Sci. **118**, 103 (1982).
[8]U. Dobler, K. Baberschke, J. Hasse, and A. Puschmann, Phys. Rev. Lett. **52**, 1437 (1984).
[9]A. G. J. DeWit, R. P. N. Bronckers, and J. M. Fluit, Surf. Sci. **82**, 177 (1979); R. P. N. Bronckers and A. G. J. DeWit, *ibid.* **112**, 133 (1981).
[10]H. Niehus and G. Comsa, Surf. Sci. **140**, 18 (1984).
[11]F. M. Chua, Y. Kuk, and P. J. Silverman, Phys. Rev. Lett. **63**, 386 (1989).
[12]R. Feidenhans'l and I. Stensgaard, Surf. Sci. **133**, 453 (1983).
[13]K. S. Liang, P. H. Fuoss, G. J. Hughes, and P. Eisenberger, in *The Structure of Surfaces,* Vol. 2 of *Spinger Series in Surface Science,* edited by M. A. Van Hove and S. Y. Tong (Springer-Verlag, Berlin, 1985), p. 246.
[14]H. P. Bonzel (private communication).
[15]D. Ghaleb and B. Perraillon, Surf. Sci. **162**, 103 (1985).
[16]F. H. P. M. Habraken and G. A. Bootsman, Surf. Sci. **87**, 333 (1979).
[17]H. Hasse, B. Hillert, and A. M. Bradshaw (unpublished).
[18]R. Feidenhans'l, F. Grey, R. L. Johnson, S. G. J. Mochrie, J. Bohr, and M. Nielsen (unpublished).
[19]D. J. Coulman, J. Wintterlin, R. J. Behm, and G. Ertl (unpublished).
[20]Y. Kuk and P. J. Silverman, Rev. Sci. Instrum. **60**, 165 (1989), and references therein.
[21]W. Telieps and E. Bauer, Surf. Sci. **200**, 512 (1988).
[22]R. Wolkow and Ph. Avouris, Phys. Rev. Lett. **60**, 1049 (1988).
[23]K. W. Jacobsen and J. K. Nørskov (unpublished).
[24]R. Courths, B. Cord, H. Wern, H. Saalfeld, and S. Hufner, Solid State Commun. **63**, 619 (1987).
[25]S. Kevan, Phys. Rev. B **28**, 4822 (1983).
[26]R. A. Bartynski, T. Gustafsson, and P. Soven, Phys. Rev. B **31**, 4745 (1985).
[27]C. T. Chen and N. V. Smith, Phys. Rev. B **35**, 5407 (1987), and unpublished.
[28]E. Kopatzki, G. Doyen, D. Drakova, and R. J. Behm, J. Microsc. **152**, 687 (1988).
[29]Y. Kuk, P. J. Silverman, and T. M. Buck, Phys. Rev. B **36**, 3104 (1987).
[30]Y. Kuk and P. J. Silverman, J. Vac. Sci. Technol. A **6**, 524 (1988).
[31]W. K. Burton, N. Cabrera, and F. C. Frank, Philos. Trans. R. Soc. London, Ser. A **243**, 299 (1951).
[32]H. L. Davis and J. R. Noonan, Surf. Sci. **126**, 245 (1983).
[33]I. Stensgaard and R. Feidenhans'l, Surf. Sci. **128**, 281 (1982).
[34]Y. Kuk and P. J. Silverman (unpublished).

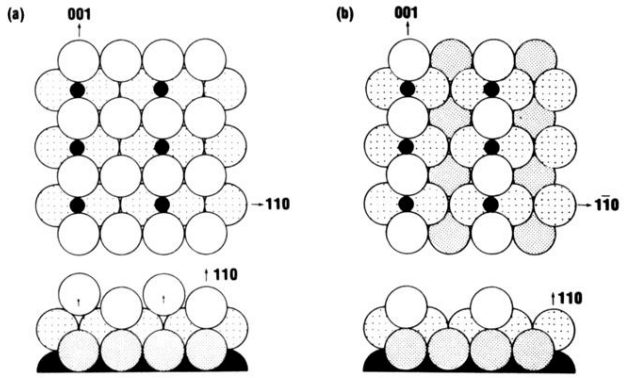

FIG. 1. Schematic diagram of the Cu(110)-O(2×1) reconstruction model. (a) Buckled-row model. (b) Missing-row model.

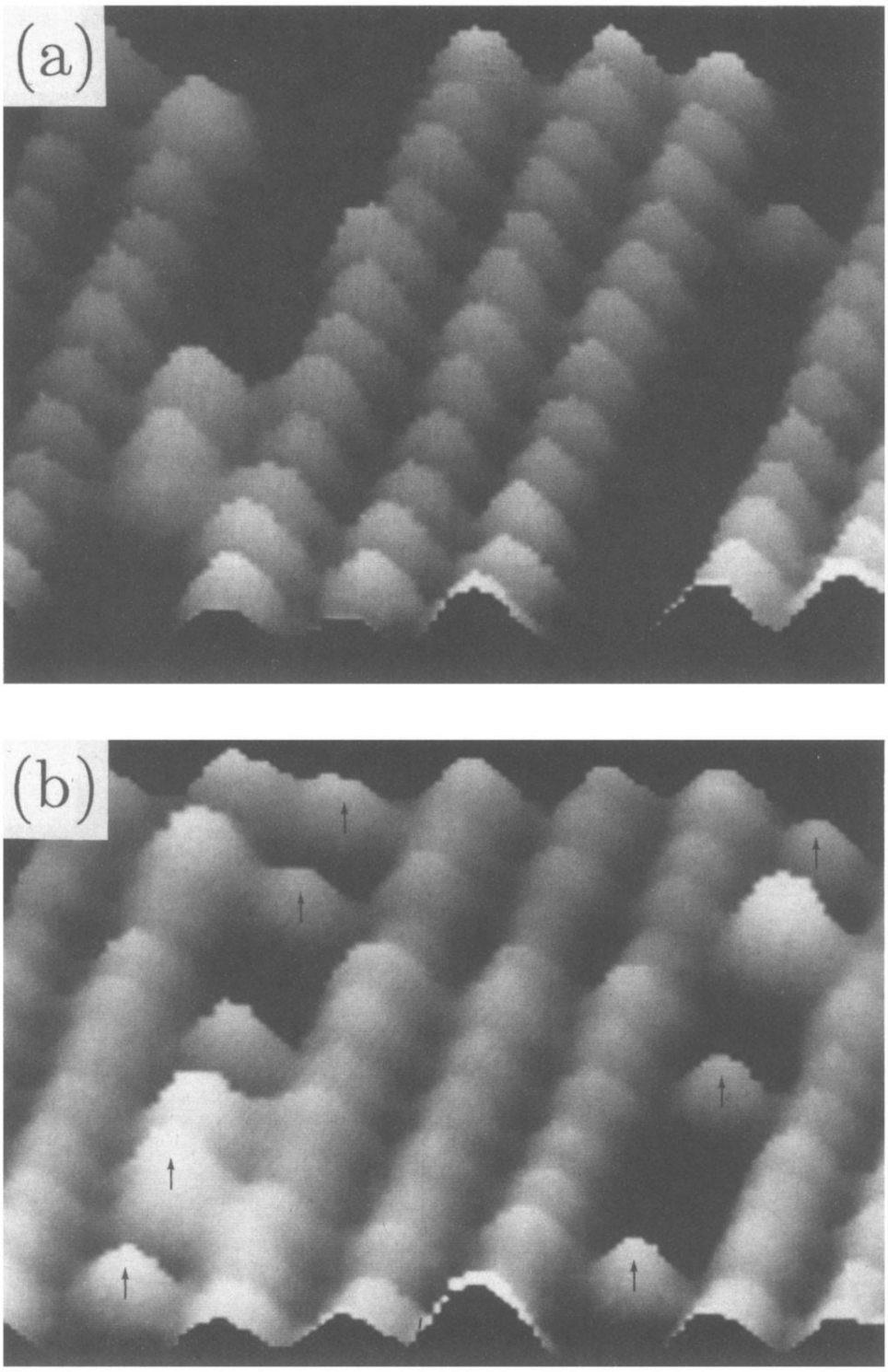

FIG. 11. 120×90-Å^2 images at (a) -1 V and (b) 2 V. The atoms indicated by arrows disappear at -1 V.

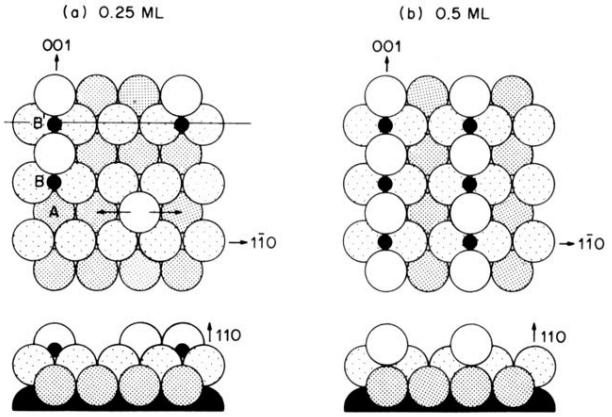

FIG. 2. Schematic diagram of the added-row model of Cu(110)-O(2×1). (a) As O atoms bind with diffusion Cu atoms (indicated by arrow) at 0.25 ML, they form an added row along ⟨001⟩. (b) At saturation coverage this model is identical to the missing-row one. A line is drawn to indicate registry, as in Fig. 4.

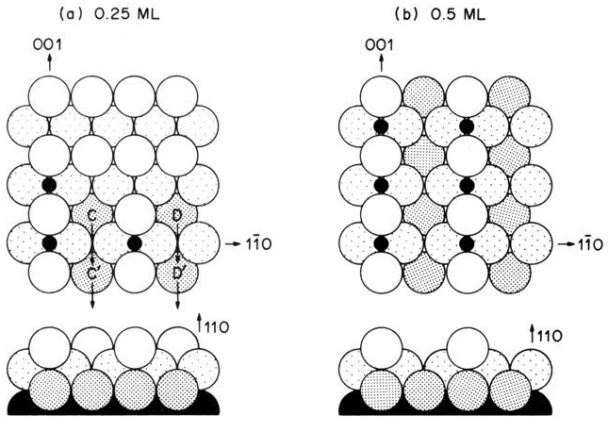

FIG. 3. Schematic diagram of the missing-row model of Cu(110)-O(2×1); (a) as three O atoms adsorb at 0.25 ML, four Cu atoms diffuse away from the area as indicated by arrows, and (b) at saturation coverage.

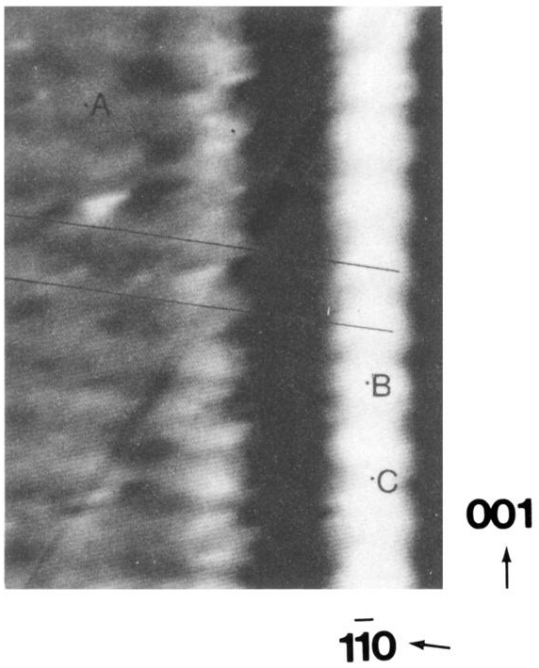

FIG. 4. 35×26-Å^2 gray-scale image at 1 V. Two solid lines are drawn to indicate the registry of the O atom with underlying Cu atoms. Spectra taken at sites *A*, *B*, and *C* are shown in Fig. 6.

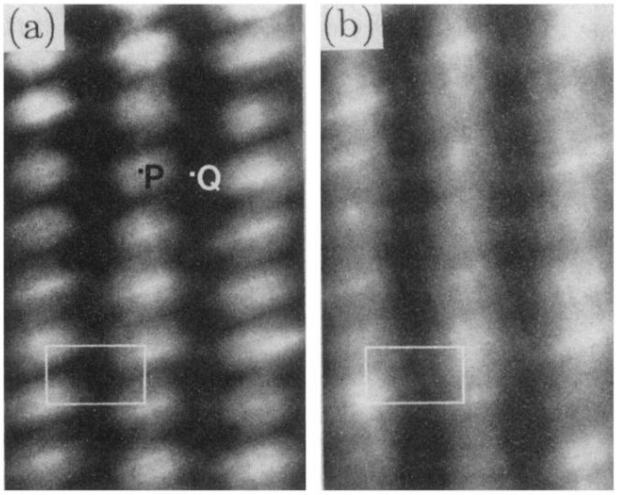

FIG. 5. 29×15.5-Å^2 gray-scale images of a Cu(110)-O(2×1) surface at (a) -1 V and (b) 2 V. (2×1) unit cells are marked.

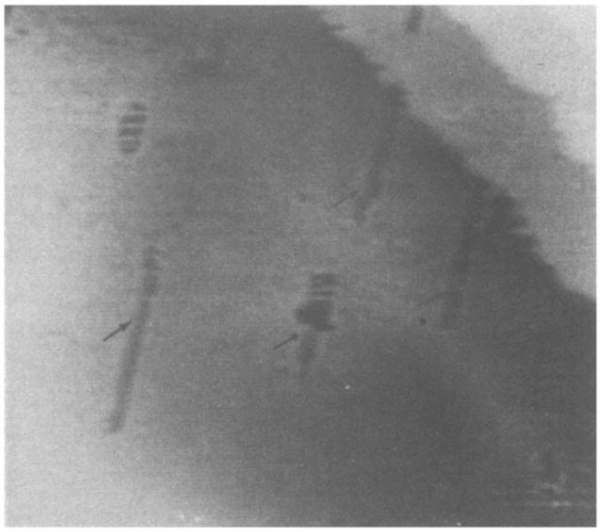

FIG. 7. 120×90-Å^2 image at $+1$ V. The O row appears as a trough due to the O-chemisorbed W tip.

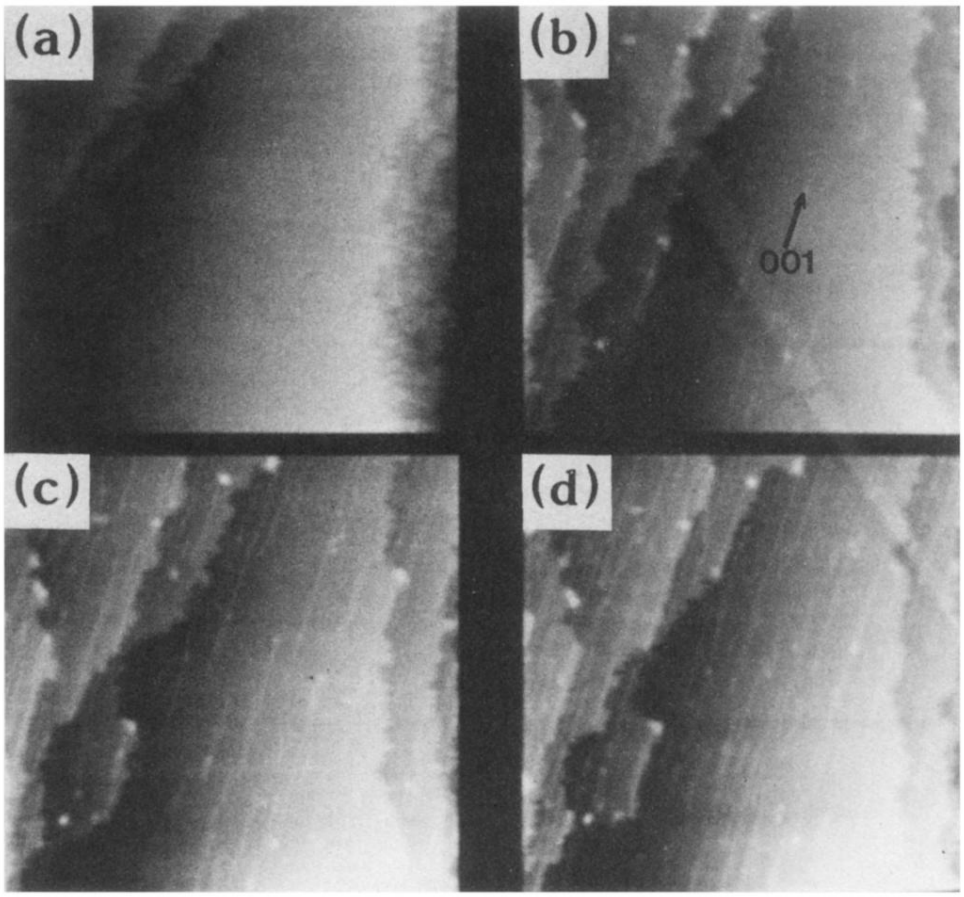

FIG. 8. 600×480-Å^2 images at −1 V on (a) clean surface, and at (b) 0.02 ML, (c) 0.06 ML, (d), 0.09 ML, (e) 0.17 ML, (f) 0.20 ML, (g) 0.30 ML, and (h) 0.40 ML coverage. Patches are indicated by small arrows. Large arrows in (e)–(g) indicate the same patch growth with increasing O coverage.

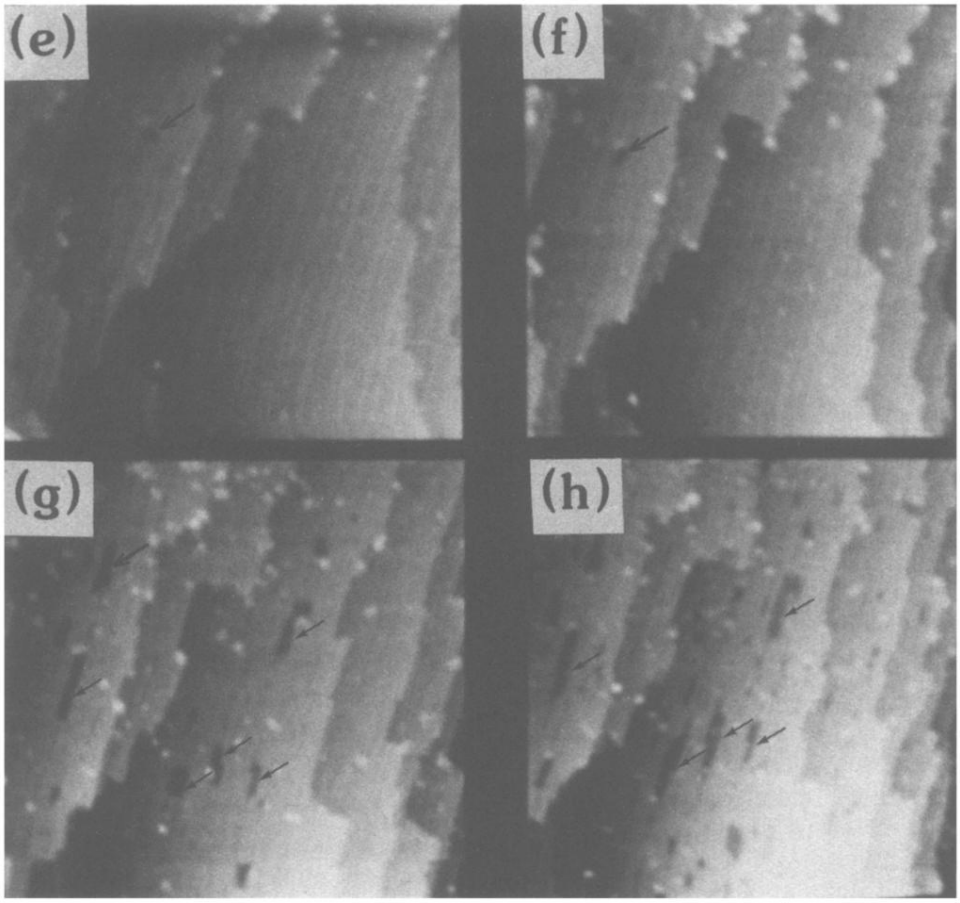

FIG. 8. (*Continued*).

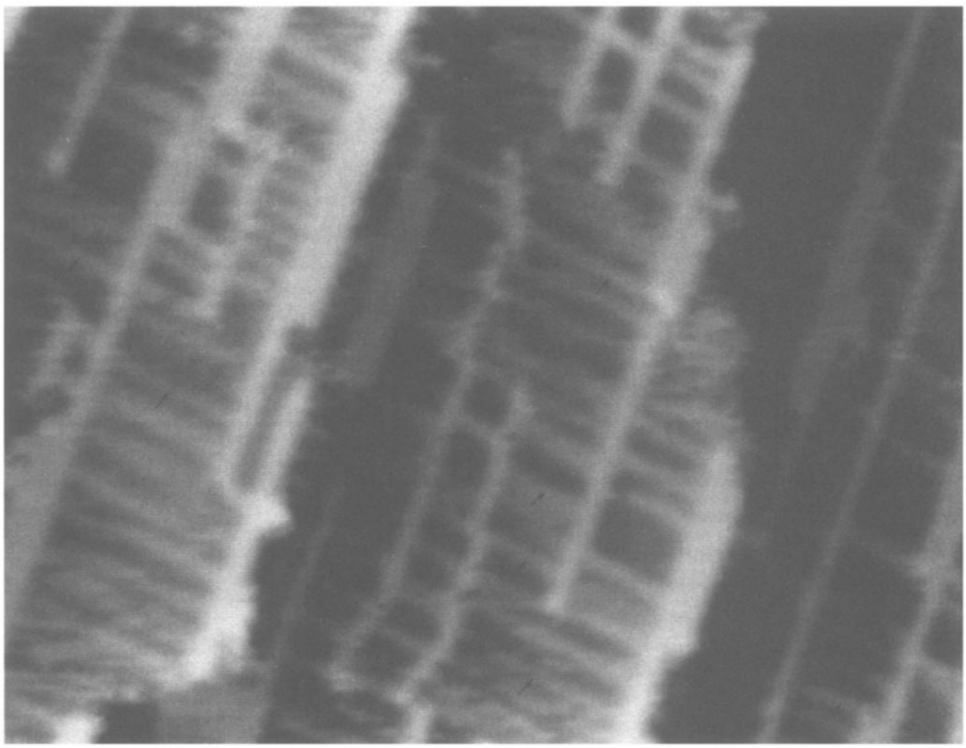

FIG. 9. 240×190-Å^2 images at 0.2 ML O. Protrusions along $\langle 1\bar{1}0 \rangle$ are shown by arrows.